encit 2020

18th Brazilian Congress of Thermal Sciences and Engineering
November 16–20, 2020 (Online)

ENC-2020-0457
INVESTIGATION ON INFLUENCE OF FORCING SCHEMES ON THEORETICAL AND SIMULATED GAS-LIQUID COEXISTENCE CURVE USING PSEUDOPOTENTIAL LATTICE BOLTZMANN METHOD

Vinícius Pessoa Mapelli
Luben Cabezas-Gómez
University of São Paulo, São Carlos School of Engineering, SP, Brazil
vinicius.mapelli@usp.br

Abstract. *Multiphase flows is a research field that draws much attention for its occurence in natural and industrial processes. Modeling these flows accurately is very challenging, and in the last few decades, pseupotential framework in lattice Boltzmann method has arisen as an interesting alternative to traditional CFD simulations due to its simplicity. In the present work, a third order analysis is used to study the behavior of gas-liquid coexistence curve for a flat planar interface. Two forcing schemes, namely, Guo* et al. *(2002) and Shan and Chen (1993), are employed in order to verify whether simulation results are well predicted by theoretical analysis. Present work analysis was compared with literature theoretical analysis, simulation and Maxwell coexistence curve results. Current theoretical coexistence curve was able to predict simulation results within 7% of accuracy while analysis from literature deviate 86% from simulation results. No differences were observed for Guo forcing scheme. Present work was also able to predict well the coexistence curve dependence of Shan-Chen scheme on relaxation time. Although applications of such schemes may be limited, a better understanding of these schemes and good theoretical approaches are key steps in order to modify and enhance lattice Boltzmann methods to simulate wider ranges of flow conditions.*

Keywords: *Lattice Boltzmann method, Pseudopotential method, gas-liquid flow, flat interface*

1. INTRODUCTION

Multiphase flows are of great interest in both academic and industrial researches due to its natural occurence in different applications, such as chemical, power-generation, heat exchanger industries, among others (Krüger *et al.*, 2017). Accurately modeling such multiphase flows is very challenging, and different approaches can be employed (Li *et al.*, 2012). In the last decades, the lattice Boltzmann method (LBM) has drawn attention for being an interesting alternative approach to simulate different problems such as porous (Guo and Zhao, 2002; Liu *et al.*, 2016) and compressible flows (Alexander *et al.*, 1992; Kataoka and Tsutahara, 2004).

Regarding multiphase flows, the pseudopotential approach proposed by Shan and Chen (1993), which incorporates an interaction potential dependent on the density, has been shown to be an effective and simple approach to multiphase and multicomponent flows. The ability to incorporate gas-liquid coexistence behavior is done through a forcing scheme, which is used to include the proposed interparticle force dependent on the pseudopotential function. A formidable number of forcing schemes has been proposed for LBM, in which most notables ones are, namely, Guo *et al.* (2002); He *et al.* (1998); Kupershtokh *et al.* (2009) and, also, the original scheme proposed in the first pseudopotential work, Shan and Chen (1993).

Such different procedures to include interparticle potential into the lattice Boltzmann equation play significant influence on stability and achievable density ratios. In fact, correctly predicting simulation results from theoretical analysis has been of major interest, since the second order analysis, commonly employed for other problems, is not able to reproduce observed simulation results. Distinct strategies have been seen in the literature to correctly predict and reproduce a thermodynamic consistent behavior in lattice Boltzmann simulations. Wagner (2006) carried out a fifth-order equilibrium analysis on to show some corrections that should be employed in order to achieve thermodynamic consistency. This analysis employed one-dimensional lattices with 3 discrete velocities (D1Q3), however, the conclusions can be extended to most common lattices used in literature, namely, D2Q9, D3Q19 and D3Q27. One of the drawbacks of such lattices is that they are second-order approximation of continuum Boltzmann equation in velocity space, and as such, they are not able to correctly recover high-order moments of distribution function. A thorough discussion and a systematic procedure for obtaining higher-order representations is shown by Shan *et al.* (2006). Philippi *et al.* (2006) also discusses how the commonly used lattices are not sufficient to correctly retrieve macroscopic behavior of energy conservation equation. They also describe a systematic procedure to obtain higher order lattices capable of retrieving thermohydrodynamic behavior. Further, these high order terms were employed to study multiphase flows (Philippi *et al.*, 2012; Mattila *et al.*, 2013). Siebert *et al.* (2014) employed D2Q17 lattice to study thermodynamic consistency using distinct equations of state and discretization of streaming step. They showed that thermodynamic consistency is only achievable by using a third order streaming step.

Even though the approach of using high order lattices has shown great results and potential, it poses some challenges regarding computational efficiency. By using a higher number of discrete velocities, numerical simulation requires a proportional higher memory usage for each lattice node. Also, as higher order representations requires values from nodes further than nearest and next-nearest neighbors, parallel implementation becomes more difficult when compared to traditional lattice schemes. For these reasons, there is still an active interest in including correction terms for tuning thermodynamic consistency and surface tension under traditional second-order lattice Boltzmann equation (LBE) framework. Kupershtokh *et al.* (2009) proposed some modifications to original Shan-Chen force, and a forcing scheme, known as exact-difference method (EDM), with free parameters to adjust liquid-gas coexistence curve. Yu and Fan (2009) proposed an additional term in order to adjust surface tension independently. They also reported that adding pseudopotential force through Shan-Chen forcing scheme leads to viscosity dependent results, whereas Guo forcing scheme presents independent results. Although they showed this numerically, they have not shown explicitly how coexistence curve is dependent on this parameter. Li *et al.* (2012) also proposed a modification to Guo forcing scheme in order to adjust coexistence curve such that final results are independent on relaxation parameter. In further works, the authors improved these methods to add a surface tension adjustment term under multiple relaxation time collision operator (Li *et al.*, 2013a; Li and Luo, 2013). Lycett-Brown and Luo (2015) analyzed the lattice Boltzmann equation for the pseudopotential method, and showed that a good agreement between theoretical values and simulation results are obtained when considering third order terms from the forcing schemes. With this knowledge, they devise a new approach capable of adjusting surface tension, interface width and coexistence curve independently. Recenlty, Kharmiani *et al.* (2019) also proposed an interaction potential approach that allows for controlling independently the liquid-gas density ration and surface tension. However, although written in common terms for second-order velocity LBE framework, it can be argued that it includes effects of nodes further than adjacent nodes due to a two-step procedure to compute gradients of interaction potential function.

In the present work, we aim to study two different forcing schemes, namely, Guo and Shan-Chen, for multiphase flows. In order to study the resulting equations, a third order analysis following what is proposed by Lycett-Brown and Luo (2015) is carried out. With that, theoretical coexistence curve can be determined for the planar interface problem. Even though many steps are shared between original procedure and present work, final theoretical coexistence curve is slightly different from what is reported in the original work. In order to validate which one produces better prediction, theoretical values are compared with Maxwell coexistence curves and with simulation results carried out under Palabos framework (Latt *et al.*, 2020). By using this methodology, main goal of this study is produce a better understanding of gas-liquid coexistence under distinct forcing scheme, since it is a key knowledge to be able to propose future enhancements to these methods.

2. METHODOLOGY

2.1 Lattice Boltzmann method

The discretized evolution of distribution function f in time, when considered an approximation of the original collision operator called BGK (Bhatnagar *et al.*, 1954), composes the traditional lattice Boltzmann method (LBM) (Krüger *et al.*, 2017), sometimes referred as LBGK method in literature. This discretized lattice Boltzmann equation (LBE) is described as follows:

$$f_i(t+\Delta t, \boldsymbol{x}+\boldsymbol{c}_i\Delta t) - f_i(t,\boldsymbol{x}) = -\frac{\Delta t}{\tau}\left[f_i - f_i^{eq}\right] + F_i, \tag{1}$$

where f_i represents the particle distribution function related with the velocity set $\boldsymbol{c_i}$, t and $\boldsymbol{x}$ are the time and space coordinates, τ is the relaxation time parameter, and Δt is the time step. The f_i^{eq} is the equilibrium distribution function, and it depends on density ρ, macroscopic velocity field $\boldsymbol{u}$ and the velocity set $\boldsymbol{c_i}$:

$$f_i^{eq} = w_i\rho\left[1+\frac{\boldsymbol{c}_i\cdot\boldsymbol{u}}{c_s^2}+\frac{1}{2}\left(\frac{\boldsymbol{c}_i\cdot\boldsymbol{u}}{c_s^2}\right)^2-\frac{\boldsymbol{u}^2}{2c_s^2}\right], \tag{2}$$

where w_i are the weights related to each of particle velocities, $\boldsymbol{c_i}$, and c_s is the lattice sound speed. For the D2Q9, lattice sound speed $c_s = 1/3$, and the weights w_i and velocities $\boldsymbol{c_i}$ are given by:

$$w_i = \begin{cases} 4/9 \text{ for } i=0 \\ 1/9 \text{ for } i=\{1\ldots4\} \\ 1/36 \text{ for } i=\{5\ldots8\} \end{cases}, \tag{3}$$

$$\boldsymbol{c}_i = \begin{cases} (0,0) \text{ for } i = 0 \\ (\pm 1, 0), (0, \pm 1) \text{ for } i = \{1 \dots 4\} \\ (\pm 1, \pm 1) \text{ for } i = \{5 \dots 8\} \end{cases}. \tag{4}$$

Density and momentum density fields can be computed through the zeroth and first order moments of the velocities distribution functions as follows:

$$\begin{aligned} \rho &= \sum_i f_i, \\ \rho \boldsymbol{u} &= \sum_i \boldsymbol{c}_i f_i. \end{aligned} \tag{5}$$

The term F_i is defined by the forcing scheme to be used. This term is responsible for taking into account the effects from external force fields in simulations. In this work, it was used the forcing scheme proposed by Shan and Chen (1993) and Guo *et al.* (2002). Given the LBM described in Eq. (1), one may describe the forcing scheme F_i as:

$$F_i = w_i \left[\frac{\boldsymbol{c}_i \cdot \boldsymbol{F}}{c_s^2} + \frac{(\boldsymbol{c}_i \cdot \boldsymbol{F})(\boldsymbol{c}_i \cdot \boldsymbol{u})}{c_s^4} - \frac{\boldsymbol{F} \cdot \boldsymbol{u}}{c_s^2} + \frac{\gamma}{2} \left(\frac{(\boldsymbol{c}_i \cdot \boldsymbol{F})^2}{c_s^4} - \frac{\boldsymbol{F} \cdot \boldsymbol{F}}{c_s^2} \right) \right], \tag{6}$$

where $\boldsymbol{F}$ is the vectorial external force field and γ is a constant which assumes $\gamma = 1 - 1/4\tau$ for Guo forcing scheme and $\gamma = \tau$ for the Shan-Chen forcing scheme.

2.2 Pseudopotential method

The pseudopotential approach for simulating multiphase flows was first proposed by Shan and Chen (1993), and the main idea can be summarized as adding the effects of an interparticle molecular force as:

$$\boldsymbol{F}_{\text{int}} = -G\psi(\boldsymbol{x}) \sum_i w_i \psi \left(\boldsymbol{x} + \boldsymbol{c}_i \Delta t \right) \boldsymbol{c}_i, \tag{7}$$

where G controls the intensity of the interparticle force and $\psi = \psi(\rho)$ is a density-dependent interaction potential. For this study, the interaction potential used is:

$$\psi = 1 - e^{-\rho}. \tag{8}$$

2.3 Macroscopic equations

It is very common in the lattice Boltzmann literature to use a second order Chapman-Enskog analysis to show that this method is capable of recovering Navier-Stokes equations. However, this methodology has been shown to be insufficent to correctly predict the behavior for multiphase flows, since the effect of the interparticle force and its derivatives become of great importance near interface regions (Wagner, 2006; Huang *et al.*, 2011; Lycett-Brown and Luo, 2015). Thus, a more precise description of macroscopic equations recovered should take into account higher order terms in the forcing scheme. A detailed derivation of such equations are found on the work of Lycett-Brown and Luo (2015). The resulting macroscopic equations are:

$$\frac{\partial \rho}{\partial t} + \nabla \cdot (\rho \hat{\boldsymbol{u}}) = 0, \tag{9a}$$

$$\frac{\partial (\rho \hat{\boldsymbol{u}})}{\partial t} + \boldsymbol{\nabla} \cdot (\rho \hat{\boldsymbol{u}} \hat{\boldsymbol{u}}) = -\boldsymbol{\nabla} p_0 + \boldsymbol{\nabla} \cdot \boldsymbol{\tau} + \boldsymbol{F} + \nabla \cdot \left[\left(\tau - \frac{1}{4} - \tau\gamma \right) \frac{\boldsymbol{F}\boldsymbol{F}}{\rho} \right] + \nabla \cdot \left[\frac{c_s^2}{12} \left[(\nabla \boldsymbol{F}) \boldsymbol{I} + \nabla \boldsymbol{F} + (\nabla \boldsymbol{F})^T \right] \right], \tag{9b}$$

where $p_0 = \rho c_s^2$ is the pressure, $\boldsymbol{\tau} = \mu \left[(\boldsymbol{\nabla} \hat{\boldsymbol{u}}) + (\boldsymbol{\nabla} \hat{\boldsymbol{u}})^T \right]$ is the viscous stress tensor, $\boldsymbol{I}$ is the identity matrix, and velocity $\hat{\boldsymbol{u}}$ is defined as:

$$\hat{\boldsymbol{u}} = \boldsymbol{u} + \frac{\boldsymbol{F} \Delta t}{2\rho}. \tag{10}$$

It is worth mentioning that last term of Eq. (9b) related to the derivatives of the force field term is not observed in a second order analysis. As the γ value for the Guo forcing scheme cancels exactly the coefficent related to the term $\boldsymbol{F}\boldsymbol{F}/\rho$, this scheme is known recover the Navier-Stokes equations up to the second order (Li *et al.*, 2012).

Dynamic viscosity μ is related to relaxation time τ through the following equation:

$$\mu = \rho c_s^2 \left(\tau - \frac{\Delta t}{2} \right). \tag{11}$$

3. Planar interface problem

A very common benchmarking problem to verify the multiphase behavior or the pseudopotential approach is the planar interface problem. A typical density profile of a flat interface problem with diffusive problem is shown in Fig. 1. In this figure, it is possible to verify the basic setup for the theorical one dimensional problem: gas and liquid densities, respectively, ρ_g and ρ_l, are set in the regions distant from the interface. Since a static condition is studied and interface is flat, mechanical pressure along the x direction is constant and equals to p_{sat}. With this simple setup, distinct characteristic of the pesudopotential method can be verified, such as, surface tension values, interface width and the theoretical coexistence curve obtained.

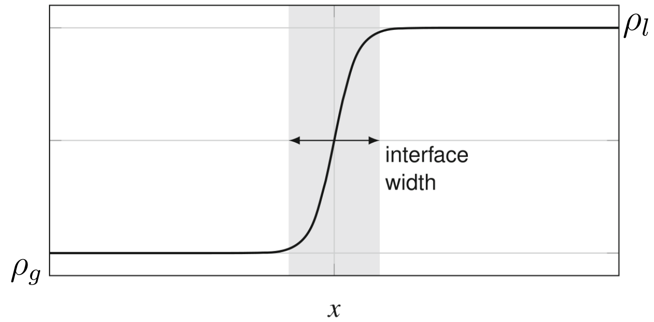

Figure 1: A typical density profile for a planar interface problem, in which two phases of a single component fluid coexist in static mechanical equilibrium (Krüger *et al.*, 2017).

Starting from Eq. (9b) and applying zero velocity condition, one may rewrite the governing equation problem as:

$$\nabla \cdot \boldsymbol{P} \equiv \boldsymbol{\nabla} \cdot \left[p_0 - \left(\tau - \frac{1}{4} - \tau\gamma \right) \frac{\boldsymbol{F}\boldsymbol{F}}{\rho} - \frac{c_s^2}{12} \left((\nabla \boldsymbol{F})\boldsymbol{I} + \nabla \boldsymbol{F} + (\nabla \boldsymbol{F})^T \right) \right] - \boldsymbol{F} = 0, \tag{12}$$

where $\boldsymbol{P}$ is known as the pressure tensor. Since the gradient of pressure tensor is zero, one may conclude that value of pressure tensor is constant along the x direction. By taking into account only the effects of the interparticle force $\boldsymbol{F}_{int}$, the pressure tensor can be written in terms of the pseudopotential function ψ. This can be done by expanding Eq. (7) in a Taylor series, substituting the result into Eq. (12) and keeping terms up to the third order (Lycett-Brown and Luo, 2015):

$$\boldsymbol{P} = \left[\rho c_s^2 + \frac{G c_s^2}{2} \psi^2 + G c_s^2 \left(\frac{c_s^2 + 1}{12} \right) |\nabla \psi|^2 + G c_s^2 \left(\frac{c_s^2 + 2}{12} \right) \psi \Delta \psi \right] \boldsymbol{I} + G c_s^2 \left[\frac{c_s^2 - 1}{6} - \frac{G c_s^2 \psi^2}{\rho} \left(\tau - \frac{1}{4} - \tau\gamma \right) \right] \nabla\psi\nabla\psi + \frac{G c_s^4}{6} \psi \nabla\nabla\psi. \tag{13}$$

With Eq. (13), the P_{xx} pressure tensor component can be written as:

$$P_{xx} = \rho c_s^2 + \frac{G c_s^2}{2} \psi^2 + G c_s^2 \left(\frac{c_s^2}{4} + \frac{1}{6} \right) \psi \frac{d^2\psi}{dx^2} + G c_s^2 \left[\frac{c_s^2}{4} - \frac{1}{12} - \frac{G c_s^2 \psi^2}{\rho} \left(\tau - \frac{1}{4} - \tau\gamma \right) \right] \left(\frac{d\psi}{dx} \right)^2. \tag{14}$$

Since $\psi = \psi(\rho)$, all derivatives in Eq. (14) can be rewritten in terms of density. This procedure leads to an ordinary differential equation with respect to $z = (d\rho/dx)^2$. Details of the algebraic manipulations are described in Krüger *et al.* (2017) and Lycett-Brown and Luo (2015). The solution of this equation yields in the theoretical coexistence curve:

$$\int_{\rho_g}^{\rho_l} e^{-G c_s^2 (\tau - 1/4 - \tau\gamma)\left(c_s^2/4 + 1/6\right)^{-1} \int^{\rho} \psi \dot{\psi} \tilde{\rho}^{-1} \, d\tilde{\rho}} \left(p_{sat} - c_s^2 \rho - \frac{G c_s^2}{2} \psi^2 \right) \frac{\dot{\psi}}{\psi^{1+\varepsilon}} d\rho = 0, \tag{15a}$$

$$p_{sat} = \rho_l c_s^2 + \frac{G c_s^2}{2} \psi(\rho_l) = \rho_g c_s^2 + \frac{G c_s^2}{2} \psi(\rho_g), \tag{15b}$$

where $\dot{\psi} = d\psi/d\rho$, and constant $\varepsilon = -2(c_s^2/4 - 1/12)/(1/6 + c_s^2/4)$. From this result, it is possible to check that theoretical coexistence curve deviates from what would be expected from the equal area Maxwell rule:

$$\int_{\rho_g}^{\rho_l} \left(p_{sat} - c_s^2 \rho - \frac{G c_s^2}{2} \psi^2 \right) \frac{d\rho}{\rho^2} = 0. \tag{16}$$

It is worth mentioning that resulting theoretical coexistence curve shown in Eq. (15) does not agree completely with results obtained by Lycett-Brown and Luo (2015), which would be written as:

$$\int_{\rho_g}^{\rho_l} \left(p_{sat} - c_s^2 \rho - \frac{G c_s^2}{2} \psi^2 \right) \frac{\dot{\psi}}{\psi^{1+\varepsilon}} d\rho = 0, \tag{17}$$

with parameter:

$$\varepsilon = \frac{-2 \left[\frac{c_s^2}{4} - \frac{1}{12} - \frac{G c_s^2 \psi^2}{\rho} \left(\tau - 1/4 - \tau\gamma \right) \right]}{\frac{1}{6} + \frac{c_s^2}{4}}. \tag{18}$$

The parameter obtained by those authors could be found by assuming that ψ^2/ρ is constant, which is not a good approximation when density varies from liquid to vapor values. However, this does not interfere in their results since they carry on their studies with Guo forcing scheme, whose corresponding γ value zero out the τ dependency of the coexistence curve, thus, both Eqs. (15) and (17) reduces to the same problem. This is not the case for forcing schemes other than Guo scheme, as it is shown for Shan-Chen scheme in the results section.

4. Results and discussions

4.1 Numerical simulations

In order to validate theoretical results shown in previous section, the flat interface problem was numerically simulating using the Palabos library (Latt *et al.*, 2020). Computational grid used are composed of 200×5 with periodic boundary conditions in all directions. Four different values of relaxation time were investigated $\tau = 0.6$, 0.8, 1.0 and 1.2. All simulations are carried out using lattice units, as commonly used in literature, and 50000 time steps as final instant. Also, distribution functions are initialized to their equilibrium values by considering zero velocity in all domain and an initial density profile with 50 lattices liquid layer at the center of the domain (Kharmiani *et al.*, 2019):

$$\rho(x) = \rho_g + \frac{\rho_l - \rho_g}{2} \left[\tanh\left(\frac{2(x-75)}{5} \right) - \tanh\left(\frac{2(x-125)}{5} \right) \right]. \tag{19}$$

4.2 Forcing scheme influence

Comparison of the coexistence curves obtained by present analysis (Eq. (15)), by Lycett-Brown and Luo procedure (Eq. (17)), Maxwell equal area rule (Eq. (16)) and simulation results are shown in Fig. 2 for both Guo and Shan-Chen forcing schemes. A constat value of relaxation time $\tau = 1$ was employed for this section. From these results, it is possible to verify a high divergence of Lycett-Brown and Luo coexistence curve (II) from the simulation results (IV) for the gas density values when Shan-Chen forcing scheme is employed. As mentioned before, this theoretical coexistence curve is obtained assuming a constant value of ψ^2/ρ, even though this value varies greatly with density from ρ_g to ρ_l. On the other hand, the coexistence curve obtained by Eq. (15) (I) correctly predicts the trend in both gas and liquid regions of the coexistence curve. As interaction strength G value decreases, theoretical and simulations results show some small divergence between them. A possible reason for this is that, as density ratio ρ_l/ρ_g increases, gradients of pseudopotential function ψ becomes higher, and terms with higher order than those considered in this analysis may play a significant role.

Regarding the Guo forcing scheme, as it was shown in the previous section, both procedures presented in the present work (Eq. (15)) (I) and Lycett-Brown and Luo (2015) (II) describes the same theoretical coexistence curve, which show good agreement with flat interface simulation results. By comparing both forcing schemes, one may notice two interesting facts. The first one is that simulated points in Guo forcing scheme presents a higher divergence with Maxwell coexistence curve (III) when compared to Shan-Chen forcing scheme. Another interesting fact to mention is that lowest stable simulation achieved with Guo forcing scheme was with interaction strength $G = -6.0$, while when Shan-Chen forcing scheme presented stable results up to $G = -8.0$.

Based on these observations, one could conclude that Shan-Chen forcing scheme is a better approach to simulate multiphase flows due to higher stability and thermodynamic consistency. However, this is not the trend most recent works have shown (Li *et al.*, 2013b, 2015; Kharmiani *et al.*, 2019). Dependence of relaxation time makes Shan-Chen forcing scheme coexistence curve much more complex and difficult to work with. Also, as relaxation time defines the dynamic viscosity, controlling thermophysical properties to match real properties becomes a more difficult task. Those are the main reasons why the current approach has been using more stable collision operators, such as multiple relaxation time (MRT), along with modified versions of Guo forcing scheme to enhance thermodynamic consitency and surface tension control.

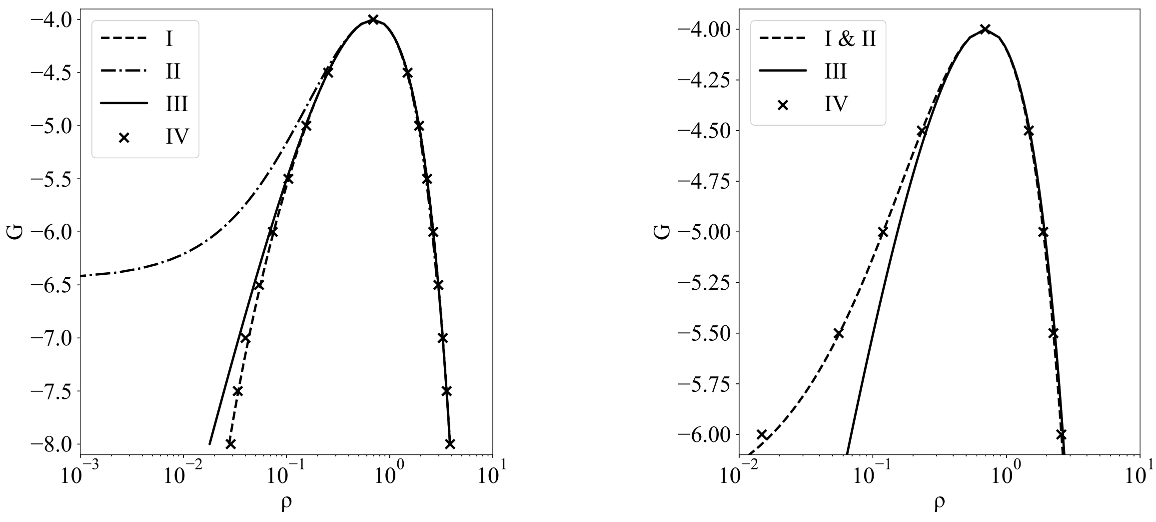

(a) Shan-Chen forcing scheme (b) Guo forcing scheme

Figure 2: Comparison of coexistence curve for Guo forcing scheme (a) and Shan-Chen forcing scheme (b) obtained by using I - the current analysis (Eq. (15)), II - Lycett-Brown and Luo (2015) coexistence curve (Eq. (17)), III - Maxwell equal area rule (Eq. (16)) and IV - simulation results.

4.3 Numerical comparison of Shan-Chen coexistence curves

Comparison of coexistence curves for the Shan-Chen forcing scheme with relaxation $\tau = 1$ obtained by present work (I), Lycett-Brown and Lou (II), Maxwell equal area rule (III) and simulation results (IV) are shown in Tab. 1, for gas densities, and in Tab. 2, for liquid densities. From these results, it is possible to quantitatively compare results of coexistence curves with simulations. The big difference between the two coexistence curves is on the gas density region. The gas densities obtained by present work procedure has shown relative differences lower than 8% from simulated values, with a maximum of 7.44% when interaction strength $G = -7.0$. When using the procedure shown in Lycett-Brown and Luo (2015) work, one may observe that estimated values grow worse as interaction strength decreases, with a maximum gas density underestimation by 86%, approximately, when compared to simulation values. For interaction strength values lower than $G = -7.0$, algorithm employed to solve Eq. (17) presented numerical instabilities and was not able to find a solution. Even so, following the curve trend for lower values of interaction strength, one may expect that absolute values of relative differences to the simulation results would be higher than 86% observed.

As for the liquid region, one may observe that both procedures present a good agreement with simulated results, with relative differences lower than 2%. However, one may conclude that present work results are better capable of predicting liquid density values, as well, since differences are lower than 0.15% for all the simulated values, while the Lycett-Brown and Luo procedure shows differences higher than 1%.

Table 1: Comparison of gas density values ρ_g obtained with Shan-Chen forcing scheme and $\tau = 1$ by: I - the current analysis (Eq. (15)), II - Lycett-Brown and Luo (2015) coexistence curve (Eq. (17)), III - Maxwell equal area rule (Eq. (16)) and IV - simulation results.

G	I	$\frac{\rho_I - \rho_{\text{sim}}}{\rho_{\text{sim}}}$	II	$\frac{\rho_{II} - \rho_{\text{sim}}}{\rho_{\text{sim}}}$	III	IV
-8.0	2.775E-02	-3.53%	-	-	1.80E-02	2.876E-02
-7.5	3.410E-02	1.35%	-	-	2.48E-02	3.365E-02
-7.0	4.302E-02	7.44%	-	-	3.44E-02	4.004E-02
-6.5	5.588E-02	3.25%	7.478E-03	-86.18%	4.83E-02	5.412E-02
-6.0	7.500E-02	2.01%	3.519E-02	-52.14%	6.89E-02	7.352E-02
-5.5	1.048E-01	0.55%	7.516E-02	-27.87%	1.01E-01	1.042E-01
-5.0	1.547E-01	-0.54%	1.362E-01	-12.44%	1.53E-01	1.555E-01
-4.5	2.512E-01	-0.88%	2.439E-01	-3.76%	2.52E-01	2.534E-01
-4.0	6.931E-01	0.00%	6.931E-01	0.00%	6.93E-01	6.931E-01

Table 2: Comparison of liquid density values ρ_l obtained with Shan-Chen forcing scheme and $\tau = 1$ by: I - the current analysis (Eq. (15)), II - Lycett-Brown and Luo (2015) coexistence curve (Eq. (17)), III - Maxwell equal area rule (Eq. (16)) and IV - simulation results.

G	I	$\frac{\rho_I - \rho_{\text{sim}}}{\rho_{\text{sim}}}$	II	$\frac{\rho_{II} - \rho_{\text{sim}}}{\rho_{\text{sim}}}$	III	IV
-8.0	3.858	-0.02%	-	-	3.848	3.859
-7.5	3.572	0.01%	-	-	3.563	3.572
-7.0	3.278	0.09%	-	-	3.269	3.275
-6.5	2.972	0.06%	2.914	-1.88%	2.964	2.970
-6.0	2.651	0.06%	2.604	-1.70%	2.645	2.649
-5.5	2.307	0.03%	2.274	-1.43%	2.303	2.307
-5.0	1.931	-0.04%	1.910	-1.11%	1.929	1.932
-4.5	1.491	-0.15%	1.483	-0.68%	1.492	1.494
-4.0	0.693	0.00%	0.693	0.00%	0.693	0.693

4.4 Relaxation time influence

Comparison of coexistence curve for the Guo forcing scheme obtained by present work procedure (Eq. (15)) (I), Lycett-Brown and Luo (Eq. (17)) (II) and Maxwell equal area rule (III) and simulation results for $\tau = 0.6$, 0.8, 1.0 and 1.2 is shown in Fig. 3. As mentioned before, both methods I and II describe the same coexistence curve, with good agreement between theoretical and simulation results. Guo forcing scheme is independent of relaxation time τ, which is an interesting characteristic since it makes it more predictable and better to control dynamic viscosity without influencing the achievable density values.

Influence of relaxation time on simulation stability is also worth mentioning from these results. As values becomes closer to the known lower limit $\tau > 0.5$, simulations becomes unstable. For instance, when $\tau = 0.6$, lowest interaction strength achievable was $G = -5.0$, while for the highest value $\tau = 1.2$, simulations with $G = -6.0$ were possible to be achieved.

The previous study is repeated for the Shan-Chen forcing scheme. Comparison between present work results (I), Maxwell equal area rule (II) and simulations for different values of relaxation time is shown in Fig. 4a. Same comparison for the procedure shown in Lycett-Brown and Luo (2015) is shown in Fig. 4b. From simulation results, it is notable how relaxation time influence greatly both stability and the achievable density ratios. For lowest value of simulation relaxation time $\tau = 0.6$, lowest stable interaction strength used was $G = -5.0$, and gas density region tends to be lower than Maxwell equal area rule. As the relaxation time increases, simulations become more stable and higher density ratios are possible to be achieved. Also, simulated gas densities migrate from values lower region of Maxwell curve to the higher one.

As for the theoretical curves, method presented in this work (a) has shown the capability to capture coexistence curves variation with relaxation time, and a good agreement is observed between simulation and theoretical values. In other hand, theoretical curve following Lycett-Brown and Luo (2015) shows a weak influence on the relaxation time, with all the curves presenting gas density values on the lower region, when compared to Maxwell equal area rule. This fact corroborates that assuming a constant value of ψ^2/ρ is a poor hypothesis for the Shan-Chen forcing scheme analysis.

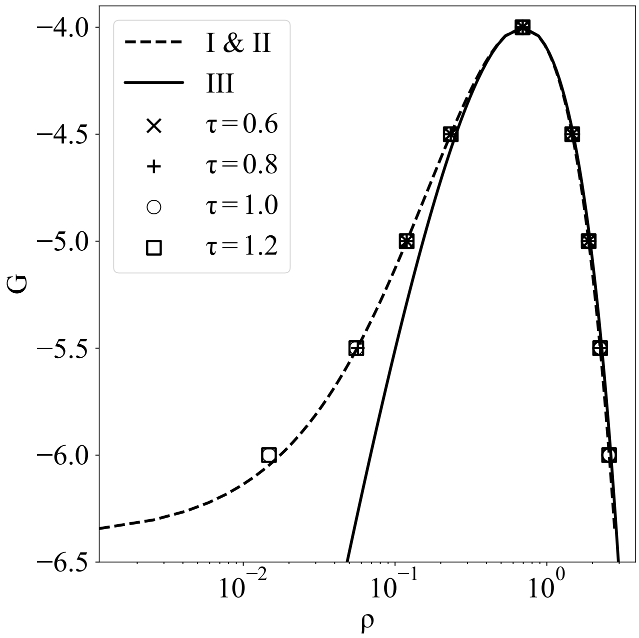

Figure 3: Theoretical coexistence curves (lines) for Guo forcing scheme obtained by: I - present work (Eq. (15)), II - Lycett-Brown and Luo approach (Eq. (17)), III - Maxwell equal area rule compared to simulated results (markers) for relaxation times $\tau = 0.6, 0.8, 1.0$ e 1.2.

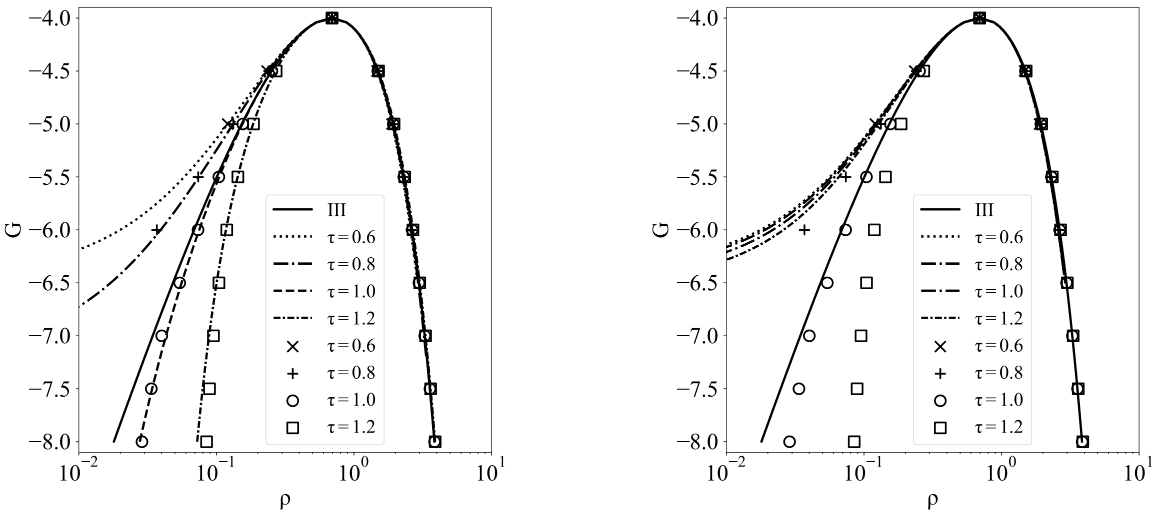

(a) (b)

Figure 4: Theoretical coexistence curves (lines) for Shan-Chen forcing scheme obtained by (a) present work (Eq. (15)), (b) Lycett-Brown and Luo approach (Eq. (17)) and Maxwell equal area rule (III) compared with simulation results (markers) for relaxation times $\tau = 0.6, 0.8, 1.0$ e 1.2.

5. Conclusions

In the present work, a study on the theoretical coexistence curve for the flat interface problem obtained considering third order terms in the forcing term is carried out. Two different forcing schemes were employed, namely, Guo and Shan-Chen schemes, under different values of relaxation time with a BGK collision operator. Also, two distinct theoretical coexistence curves are employed to analyze results: from the analysis from the current work and following the curve present in the Lycett-Brown and Luo (2015) work. These results are compared with lattice Boltzmann simulations and coexistence curve obtained by Maxwell equal area rule. Conclusions drawn from these studies can be summarized in the following points:

- When comparing simulations, Guo forcing scheme were more unstable than when Shan-Chen scheme were employed, thus, achieving higher density ratios. As for the simulated results of coexistence curve, Shan-Chen scheme presents a strong relation with relaxation time, while it plays no significant role on Guo scheme simulations. As it is more predictable and easier to be modified, Guo scheme has been chosen as a better approach to enhance thermodynamic consistency of methods in most recent works in literature.

- Regarding theoretical analysis, both procedures shown in the present work and by Lycett-Brown and Luo (2015) produces same results when Guo forcing scheme is used. As those authors used this scheme to present their improved forcing term, inconsistency found on their theoretical coexistence curve is not significant for their results.

- When comparing both procedures to analyze Shan-Chen scheme results, significant differences are observe, specially, in the gas density regions. For relaxation time $\tau = 1$, Lycett-Brown and Luo procedure presented results with a maximum underestimation of 86.18% when compared to simulations. By using present work analysis, maximum relative difference observed was 7.44%.

- Also, both theoretical anaylis procedures were compared under four relaxation times $\tau = 0.6$, 0.8, 1.0 and 1.2. By using procedure from literature, a small influence of relaxation time is observed and theoretical results are not able to correctly predict the behavior from literature. Meanwhile, theoretical coexistence curve presented in this work has shown a great dependence of relaxation time and good agreement with variations for different values.

- Both schemes under conditions studied were not able to reproduce Maxwell coexistence curve, with a great divergence in the gas region. Guo forcing scheme tends to underestimates gas density values. On the other hand, Shan-Chen shows same trend for relaxation times $0.6 \leq \tau \leq 0.8$, while it superestimates these values for $\tau > 1.0$.

- From previous item, one may conclude it could be possible to tune simulated coexistence curve to achieve thermodynamic consistency results by searching a relaxation parameter in the region $0.8 \leq \tau \leq 1.0$. Even so, as relaxation parameter is used to determine dynamic viscosity, such approach is not endorsed by physical arguments and is not suitable to be generalized.

6. ACKNOWLEDGEMENTS

The authors acknowledge the support received from CAPES (Coordination for the Improvement of Higher Education Personnel, Finance Code 001), from CNPq (National Council for Scientific and Technological Development, process 304972/2017-7) and FAPESP (São Paulo Foundation for Research Support, 2016/09509-1 and 2018/09041-5), for developing research that have contributed to this study.

7. REFERENCES

Alexander, F.J., Chen, H., Chen, S. and Doolen, G., 1992. "Lattice Boltzmann model for compressible fluids". *Physical Review A*, Vol. 46, No. 4, p. 1967.

Bhatnagar, P.L., Gross, E.P. and Krook, M., 1954. "A model for collision processes in gases I". *Physical Review*, Vol. 94, No. 3.

Guo, Z. and Zhao, T., 2002. "Lattice Boltzmann model for incompressible flows through porous media". *Physical Review E*, Vol. 66, No. 3, p. 036304.

Guo, Z., Zheng, C. and Shi, B., 2002. "Discrete lattice effects on the forcing term in the lattice Boltzmann method". *Physical Review E*, Vol. 65, No. 4, p. 046308.

He, X., Shan, X. and Doolen, G.D., 1998. "Discrete Boltzmann equation model for nonideal gases". *Physical Review E*, Vol. 57, No. 1, p. R13.

Huang, H., Krafczyk, M. and Lu, X., 2011. "Forcing term in single-phase and Shan-Chen-type multiphase lattice Boltzmann models". *Physical Review E*, Vol. 84, No. 4, p. 046710.

Kataoka, T. and Tsutahara, M., 2004. "Lattice Boltzmann model for the compressible navier-stokes equations with flexible specific-heat ratio". *Physical Review E*, Vol. 69, No. 3, p. 035701.

Kharmiani, S.F., Niazmand, H. and Passandideh-Fard, M., 2019. "An alternative high-density ratio pseudo-potential lattice Boltzmann model with surface tension adjustment capability". *Journal of Statistical Physics*, Vol. 175, No. 1, pp. 47–70.

Krüger, T., Kusumaatmaja, H., Kuzmin, A., Shardt, O., Silva, G. and Viggen, E.M., 2017. "The lattice Boltzmann method". *Springer International Publishing*, Vol. 10, pp. 978–3.

Kupershtokh, A., Medvedev, D. and Karpov, D., 2009. "On equations of state in a lattice Boltzmann method". *Computers & Mathematics with Applications*, Vol. 58, No. 5, pp. 965–974.

Latt, J., Malaspinas, O., Kontaxakis, D., Parmigiani, A., Lagrava, D., Brogi, F., Belgacem, M.B., Thorimbert, Y., Leclaire, S., Li, S. and et al., 2020. "Palabos: Parallel lattice Boltzmann solver". *Computers and Mathematics with Applications*.

Li, Q., Kang, Q., Francois, M., He, Y. and Luo, K., 2015. "Lattice Boltzmann modeling of boiling heat transfer: The boiling curve and the effects of wettability". *International Journal of Heat and Mass Transfer*, Vol. 85, p. 787–796.

Li, Q., Luo, K.H. and Li, X.J., 2013a. "Lattice Boltzmann modeling of multiphase flows at large density ratio with an improved pseudopotential model". *Physical Review E*, Vol. 87, No. 5.

Li, Q., Luo, K.H. and Li, X.J., 2013b. "Lattice Boltzmann modeling of multiphase flows at large density ratio with an improved pseudopotential model". *Physical Review E*, Vol. 87, No. 5.

Li, Q., Luo, K.H. and Li, X.J., 2012. "Forcing scheme in pseudopotential lattice Boltzmann model for multiphase flows". *Physical Review E*, Vol. 86, No. 1, p. 016709.

Li, Q. and Luo, K.H., 2013. "Achieving tunable surface tension in the pseudopotential lattice Boltzmann modeling of multiphase flows". *Physical Review E*, Vol. 88, No. 5, p. 53307.

Liu, H., Kang, Q., Leonardi, C.R., Schmieschek, S., Narváez, A., Jones, B.D., Williams, J.R., Valocchi, A.J. and Harting, J., 2016. "Multiphase lattice Boltzmann simulations for porous media applications". *Computational Geosciences*, Vol. 20, No. 4, pp. 777–805.

Lycett-Brown, D. and Luo, K.H., 2015. "Improved forcing scheme in pseudopotential lattice Boltzmann methods for multiphase flow at arbitrarily high density ratios". *Physical Review E*, Vol. 91, No. 2, p. 023305.

Mattila, K.K., Siebert, D.N., Hegele, L.A. and Philippi, P.C., 2013. "High-order lattice-Boltzmann equations and stencils for multiphase models". *International Journal of Modern Physics C*, Vol. 24, No. 12, pp. 1–4.

Philippi, P.C., Hegele, L.A., Dos Santos, L.O. and Surmas, R., 2006. "From the continuous to the lattice Boltzmann equation: The discretization problem and thermal models". *Physical Review E*, Vol. 73, No. 5, pp. 1–12.

Philippi, P.C., Mattila, K.K., Siebert, D.N., Dos Santos, L.O., Júnior, L.A. and Surmas, R., 2012. "Lattice-Boltzmann equations for describing segregation in non-ideal mixtures". *Journal of Fluid Mechanics*, Vol. 713, pp. 564–587.

Shan, X. and Chen, H., 1993. "Lattice Boltzmann model for simulating flows with multiple phases and components". *Physical Review E*, Vol. 47, No. 3, p. 1815.

Shan, X., Yuan, X.F. and Chen, H., 2006. "Kinetic theory representation of hydrodynamics: a way beyond the Navier-Stokes equation". *Journal of Fluid Mechanics*, Vol. 550, pp. 413–441.

Siebert, D.N., Philippi, P.C. and Mattila, K.K., 2014. "Consistent lattice Boltzmann equations for phase transitions". *Physical Review E*, Vol. 90, No. 5, pp. 1–15.

Wagner, A.J., 2006. "Thermodynamic consistency of liquid-gas lattice Boltzmann simulations". *Physical Review E*, Vol. 74, No. 5.

Yu, Z. and Fan, L.S., 2009. "An interaction potential based lattice Boltzmann method with adaptive mesh refinement (AMR) for two-phase flow simulation". *Journal of Computational Physics*, Vol. 228, No. 17, pp. 6456–6478.

8. RESPONSIBILITY NOTICE

The authors are solely responsible for the printed material included in this paper.